Journal of Experimental Botany, Vol. 69, No. 22 pp. 5433–5443, 2018
doi:10.1093/jxb/ery296 Advance Access publication 14 August 2018
This paper is available online free of all access charges (see https://academic.oup.com/jxb/pages/openaccess for further details)

RESEARCH PAPER

Mesophyll conductance in cotton bracts: anatomically determined internal CO_2 diffusion constraints on photosynthesis

Jimei Han[1], Zhangying Lei[1], Jaume Flexas[2], Yujie Zhang[1], Marc Carriquí[2], Wangfeng Zhang[1] and Yali Zhang[1,*]

[1] The Key Laboratory of Oasis Eco-agriculture, Xinjiang Production and Construction Group, Shihezi University, Shihezi, 832003, P.R. China

[2] Research Group in Plant Biology under Mediterranean Conditions, Universitat de les Illes Balears-Instituto de Agroecología y Economía del Agua (INAGEA), Palma 07122, Illes Balears, Spain

* Correspondence: zhangyali_cn@foxmail.com or zhangyali_shzu@163.com

Received 7 May 2018; Editorial decision 6 August 2018; Accepted 10 August 2018

Editor: Susanne von Caemmerer, Australian National University, Australia

Abstract

Mesophyll conductance (g_m) has been shown to affect photosynthetic capacity and thus the estimates of terrestrial carbon balance. While there have been some attempts to model g_m at the leaf and larger scales, the potential contribution of g_m to the photosynthesis of non-leaf green organs has not been studied. Here, we investigated the influence of g_m on photosynthesis of cotton bracts and how it in turn is influenced by anatomical structures, by comparing leaf palisade and spongy mesophyll with bract tissue. Our results showed that photosynthetic capacity in bracts is much lower than in leaves, and that g_m is a limiting factor for bract photosynthesis to a similar extent to stomatal conductance. Bract and the spongy tissue of leaves have lower mesophyll conductance than leaf palisade tissue due to the greater volume fraction of intercellular air spaces, smaller chloroplasts, lower surface area of mesophyll cells and chloroplasts exposed to leaf intercellular air spaces and, perhaps, lower membrane permeability. Comparing bracts with leaf spongy tissue, although bracts have a larger cell wall thickness, they have a similar g_m estimated from anatomical characteristics, likely due to the cumulative compensatory effects of subtle differences in each subcellular component, especially chloroplast traits. These results provide the first evidence for anatomical constraints on g_m and photosynthesis in non-leaf green organs.

Keywords: Anatomical structures, CO_2 diffusion, cotton bracts, mesophyll conductance, non-leaf green organs, stomatal conductance.

Introduction

To reach the sites of carboxylation within chloroplasts of leaves of C_3 plants, CO_2 must diffuse through stomata and mesophyll. Stomatal CO_2 diffusion occurs from the ambient air just outside the leaf to the substomatal cavities, while mesophyll CO_2 diffusion occurs from the substomatal cavities to just outside the mesophyll cell wall (i.e. gas phase resistance) and to all the cell structures (cell wall, plasma membrane, cytoplasm, chloroplast envelope membranes, and stroma) that CO_2 must necessarily pass through to reach the carboxylation center (i.e. liquid phase resistances; Evans *et al.*, 1994, 2009). Although CO_2 diffusion through the leaf has been widely studied, this fairly complex process is not fully understood yet (Evans *et al.*,

2009; Flexas *et al.*, 2012; Tosens *et al.*, 2012*b*). Many studies have shown that mesophyll conductance (g_m) significantly limits photosynthesis and often can be the main limitation to photosynthesis (Flexas *et al.*, 2008; Tosens *et al.*, 2012*b*; Galmés *et al.*, 2014; Peguero-Pina *et al.*, 2017). In the gas phase conductance, CO_2 diffusion through intercellular air spaces may be hindered by leaf thickness, mesophyll cell shape, relative distribution of palisade and spongy tissue (Evans *et al.*, 2009), and the volume fraction of intercellular air spaces (f_{ias}) (Syvertsen *et al.*, 1995; Terashima *et al.*, 1995). Regarding the liquid phase conductance, it is mainly constrained by the cell wall thickness (T_{cw}), the chloroplast dimensions, and the mesophyll and chloroplast surface area exposed to leaf intercellular air spaces (S_m/S and S_c/S) (Evans *et al.*, 1994, 2009; Tosens *et al.*, 2012*b*; Tomás *et al.*, 2013). These anatomical structures have been observed to strongly differ between different species (Tomás *et al.*, 2013; Peguero-Pina *et al.*, 2016) or even within the same species growing under complex and variable growth environments (Terashima *et al.*, 2011; Tosens *et al.*, 2012*a*).

Mesophyll conductance (g_m) is important in setting the plant photosynthetic capacity. However, the neglect of CO_2 drawdown from the substomatal cavities to chloroplasts in the photosynthetic model at the leaf level (Niinemets, 2007) and global carbon cycle model (Sun *et al.*, 2014), by using intercellular CO_2 concentration (C_i) instead of chloroplastic CO_2 concentration (C_c), results in an underestimation of the biochemical parameters, particularly the maximum carboxylation rate (V_{cmax}) and maximum electron transport rate (J_{max}). To avoid such underestimation, some modeling studies have focused on g_m and estimated photosynthetic parameters using C_c at the leaf (Ethier and Livingston, 2004; Sharkey *et al.*, 2007; Gu *et al.*, 2010; Sharkey, 2016) and whole canopy scales (Sun *et al.*, 2014).

It has been shown that non-leaf green organs are also an important source of assimilated carbon at the ecological and agricultural scales (Tambussi *et al.*, 2007; Redondo-Gómez *et al.*, 2010; Pengelly *et al.*, 2011; Hu *et al.*, 2012; Jia *et al.*, 2015; Zhang *et al.*, 2015), and thus make a considerable contribution to the terrestrial carbon exchange. However, the importance of the mesophyll diffusion limitation for photosynthesis has yet to be studied in the non-leaf green organs.

Currently, in agricultural production, it has been demonstrated that cotton bracts, non-leaf green organs that cover cotton fruits, make a significant contribution to cotton carbon gain especially in the later growth stages (Hu *et al.*, 2012). A higher water use efficiency (Hu *et al.*, 2013) and drought tolerance (Zhang *et al.*, 2015) in bracts than in leaves was also reported. However, no research has focused on the relationship between these photosynthetic characteristics and the property of CO_2 diffusion, especially mesophyll CO_2 diffusion in the bracts. Without explicit consideration of g_m, some photosynthetic parameters in bracts would have been underestimated just like in the leaves. Generally, the difference in morphological and anatomical structures between leaves and bracts is obvious (Fig. 1; Hu *et al.*, 2012). But the difference in internal mesophyll structure is still not clear. Research has shown that in the cotton bracts there is only one type of photosynthetic tissue, which is similar to the spongy tissue of the leaf.

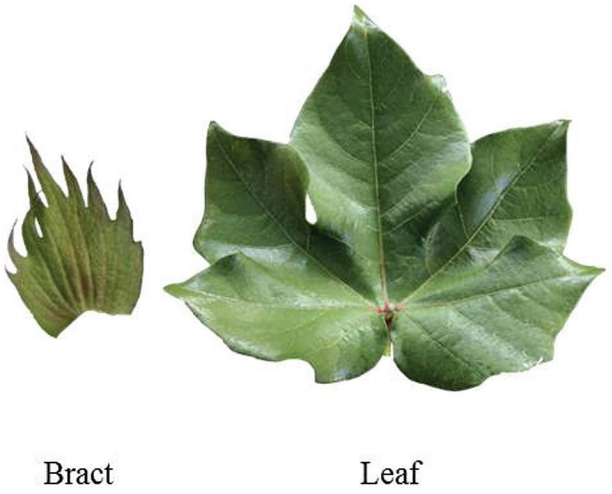

Fig. 1. A bract and a leaf from the cotton plant.

However, there are smaller and less numerous chloroplasts and more loose tissue in the spongy tissue, from which we speculate there is a larger mesophyll limitation in the bract than in the leaf. To the best of our knowledge, no previous study has analysed the effect of internal structures of palisade and spongy tissues on mesophyll diffusion of CO_2. To fill this gap, cotton leaves and bracts were studied and we compared the anatomy of palisade and spongy tissue structures with that of bracts. The aims of the study were (i) to determine if bracts are constitutively more limited than leaves for CO_2 diffusion; (ii) to reveal if the different types of tissues lead to a difference in mesophyll diffusion between the leaf and the bract; and (iii) to quantify the contribution of mesophyll structures to setting differences in g_m and photosynthesis between leaves and bracts.

Materials and methods

Plant material

Cotton (*Gossypium hirsutum* L. 'Xinluzao 45') plants were grown at an experimental field of Shihezi Agricultural College, Shihezi University, Xinjiang, China (45°19′N, 86°03′E). Before sowing, drip irrigation tubes were installed beneath the plastic film, which supplied water for the cotton. Seeds were sown on 21 April 2015 in rows 12 cm apart at a plant density of 1.8×10^5 ha^{-1}. The plots were fertilized before sowing with 240 kg N ha^{-1} (urea), 170 kg P_2O_5 ha^{-1} [$(NH_4)_3PO_4$], and 1500 kg ha^{-1} organic fertilizer (235 g kg^{-1} organic matter, 18 g kg^{-1} total N, 14 g kg^{-1} total P, and 22 g kg^{-1} total K). An additional 120 kg N ha^{-1} (urea) was applied by drip irrigation during the growing seasons. Weeds and pests were controlled in the field using standard management practices. At peak bolling stage (100–110 days after sowing), the topmost fully expanded leaf on the main stem and bract on the fruit branch of the cotton were selected for the experiment. Meteorological data during the growing season are shown in Supplementary Fig. S1 at *JXB* online.

Gas exchange and chlorophyll fluorescence

Gas exchange and chlorophyll fluorescence were measured simultaneously on the main leaves and bracts, using an open gas-exchange system (Li-6400; Li-Cor, Inc., Lincoln, NE, USA) connected to a leaf fluorometer chamber (Li-6400-40; Li-Cor Inc.). The bolls were detached from the bracts so as to be able to clamp the bract to obtain the CO_2 and light response curves. Leaf temperature was set to 30 °C. The vapor pressure deficit (VPD) was between 2 and 3 kPa and the flow rate was set

at 300 μmol s^{-1}. The ratio of red:blue light was set to 90:10% PPFD to maximize stomatal aperture. CO_2 concentration in the Li-6400 leaf chamber was provided by a CO_2 cylinder and maintained constant at 400 μmol CO_2 mol^{-1}. Light-response curves were obtained under the light intensities 2000, 1800, 1500, 1200, 1000, 800, 500, 300, 200, 150, 100, 50, and 0 μmol m^{-2} s^{-1} for leaves and 1500, 1200, 1000, 800, 500, 300, 200, 150, 100, 50, and 0 μmol m^{-2} s^{-1} for bracts. CO_2-response curves in light saturating conditions were obtained by first determining the parameters at 2000 μmol m^{-2} s^{-1} photosynthetically active photon flux density (PPFD) for leaves and at 1000 μmol m^{-2} s^{-1} for bracts (see Fig. 2B for A_N–PAR curves confirming light saturating conditions for both leaves and bracts). Photosynthesis was induced with an ambient CO_2 concentrations (C_a) of 400 μmol mol^{-1} and 21% O_2 surrounding the leaf. Once steady state was reached (usually 20 min after clamping the leaf), data were recorded. Immediately after, the air inlet pipe was connected to a 2% O_2 and 98% N_2 medical gas bag, and a CO_2-response curve (net assimilation rate (A_N)–C_i curve) was obtained. After that, the Li-COR inlet was disconnected from N_2 medical gas bag (i.e. air with 21% O_2 was supplied again to the plant). After reaching steady state, another A_N–C_i curve was obtained. In regard to the A_N–C_i curve, gas exchange and chlorophyll fluorescence were first measured at C_a of 400 μmol mol^{-1}; then C_a was decreased stepwise to 50 μmol mol^{-1}. Upon completion of measurements at low C_a, C_a was returned to 400 μmol mol^{-1} to restore the original A_N. Then C_a was increased stepwise to complete the curve. The number of different C_a values used for the curves was 12, and the time interval between two consecutive measurements at different C_a was restricted to 2–4 min, so that each curve was completed in 30–50 min. The actual photochemical efficiency of photosystem II (Φ_{PSII}) was determined by measuring steady state fluorescence (F_s) and maximum fluorescence during a light-saturating pulse of ca. 8000 μmol m^{-2} s^{-1} (F_m'):

$$\Phi_{PSII} = \frac{F_m' - F_S}{F_m'} \quad (1)$$

The electron transport rate (J_{flu}) was then calculated as:

$$J_{flu} = \Phi_{PSII} \times PPFD \times \alpha \times \beta \quad (2)$$

Where PPFD is the photosynthetically active photon flux density, α is leaf absorptance and β reflects the partitioning of absorbed quanta between photosystems II and I (PSI and PSII). α was assumed to be 0.85 and β to be 0.5. Because numerous studies have shown that the estimation of J_{flu} is affected by PSI and the signal-to-noise ratio in the determination of F_m' at high light, the electron transport rate from gas exchange under 2% O_2 conditions (J_A) was used to calibrate J_{flu} (see Pons *et al.*, 2009 for details).

g_m was estimated by the variable *J* method (Harley *et al.*, 1992*a*) as:

$$g_{m(Harley)} = \frac{A_N}{C_i - \frac{\Gamma\star \times [J_{flu} + 8(A_N + R_d)]}{J_{flu} - 4(A_N + R_d)}} \quad (3)$$

where $\Gamma\star$ is the CO_2 compensation point in the absence of mitochondrial respiration and R_d is day respiration. A_N and C_i were taken from gas-exchange measurements at saturating light and the value of $\Gamma\star$ (44.04) at 30 °C from Bernacchi *et al.* (2002) used for the variable *J* methods of calculating g_m:

$$\Gamma^\star = \exp\left(13.49 - \frac{24460}{8.314 \times (273.15 + T_L)}\right)$$

where T_L is the leaf temperature (°C). R_d was assumed to be half of the measured dark respiration (R_n, R_d=R_n/2) (Villar *et al.*, 1995; Niinemets *et al.*, 2005). R_n was determined by gas exchange (Li-6400), after plants had been dark-adapted for more than half an hour in the evening. CO_2 leakage of the leaf cuvette was determined by performing A_N–C_i response curves with photosynthetically inactive leaves and bracts enclosed in the leaf chamber (obtained by heating the leaves until no variable chlorophyll fluorescence was observed), and used to correct measured leaf fluxes (Flexas *et al.*, 2007).

Estimation of g_m by A_N–C_i curve fitting

The curve-fitting method introduced by Sharkey (2016) was used to obtain an alternative estimate of g_m. This method is based on changes in the curvature of A_N–C_i response curves due to a finite g_m. By non-linear curve fitting minimizing the sum of squared model deviations from the data, g_m can be estimated from observed data. The same data were used for estimation of g_m by the methods of Sharkey (2016) and Harley *et al.* (1992*a*).

Estimation of V_{cmax} and J_{max}

The A_N–C_c curves were fitted based upon the model of Farquhar *et al.* (1980), which was later modified and developed by Harley *et al.* (1992*a*,*b*). According to the biochemical model, A_N can be expressed as:

$$A_N = V_c - 0.5V_o - R_d = \min\{A_c, A_j, A_p\} \quad (4)$$

With

$$A_c = \frac{V_{cmax} \times (C_c - \Gamma^\star)}{C_c + K_c \times (1 + \frac{O}{K_o})} - R_d \quad (5)$$

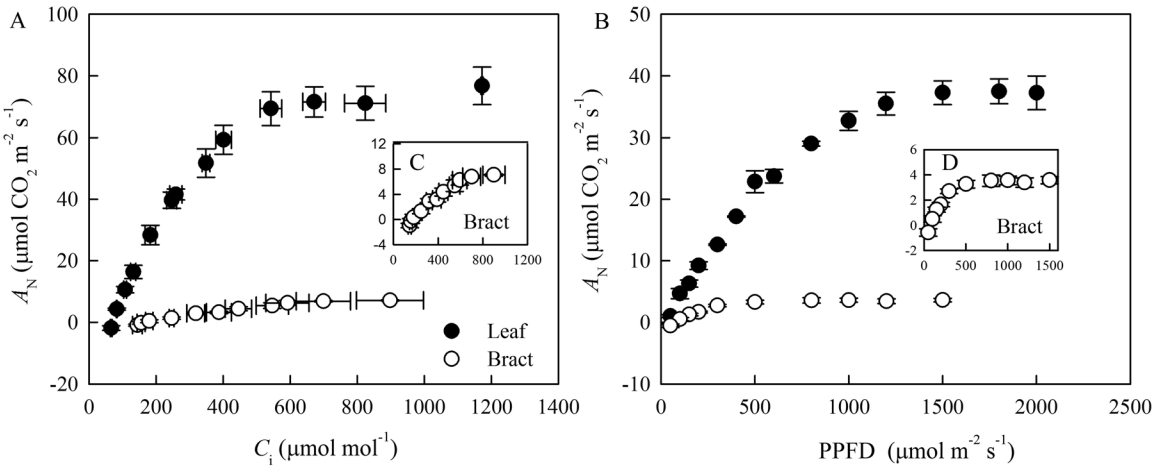

Fig. 2. Net CO_2 assimilation rate (A_N) expressed on the basis of leaf area as a function of intercellular CO_2 concentration (C_i) (A) and photosynthetically active photon flux density (PPFD) (B) in cotton leaves and bracts. Bracts data are also shown in the insets (C, D). Values are means±SE.

$$A_j = \frac{J_{max} \times (C_c - \Gamma^\star)}{4C_c + 8\Gamma^\star} - R_d \quad (6)$$

where A_c, A_j, and A_p are the net CO_2 assimilation rate limited by Rubisco, ribulose 1,5-bisphosphate (RuBP), and triose phosphate use (TPU), respectively. V_c and V_o are rates of carboxylation and oxygenation of Rubisco. O is the O_2 concentration at the sites of carboxylation within chloroplasts. K_c and K_o are Michaelis–Menten constants for carboxylation and oxygenation, respectively (Bernacchi *et al.*, 2002). Best-fit values of the parameters J_{max} and V_{cmax} were obtained using the whole curve data points (i.e. Eqn 4) rather than a portion of the curve according to 'method I' of Miao *et al.* (2009).

Electron microscopy

Leaf and bract samples (4 mm×1.5 mm) were fixed by infiltration of 2.5% glutaraldehyde and 3% paraformaldehyde in 0.1 mol l^{-1} phosphate buffer (pH 7.2) under vacuum. Leaf samples were fixed again in 1% osmium tetroxide overnight and dehydrated in a graded acetone series and embedded in Spurr's resin. Semi-thin leaf cross-sections of 4 μm for light microscopy and ultra-thin (80 nm) cross-sections were prepared with an ultramicrotome (Leica Ultracut, Germany). The sections for light microscopy were stained with toluidine blue. Ultra-thin cross-sections for transmission electron microscopy were stained with uranyl acetate and lead citrate double staining, observed under an electron microscope (TEM HT7700, Japan), and electron micrographs were taken with a digital camera (BH-2, Olympus). Each anatomical trait per replicate was measured 6–10 times. It should be noted that electron micrographs of palisade and spongy tissues were taken and then quantified according to the below methods and formulas.

The surface of mesophyll cells and chloroplasts exposed to leaf intercellular air spaces (S_m/S and S_c/S) were calculated following the method of Syvertsen *et al.* (1995) as:

$$\frac{S_m}{S} = \frac{L_{mes} \times F}{W} \quad (7)$$

where L_{mes} is the total length of mesophyll cells facing the intercellular air space in the palisade tissue or spongy tissue section, F is the curvature correction factor that depends on the shape of the cells (Thain, 1983; Evans *et al.*, 1994), and W is the width of the section measured.

$$\frac{S_c}{S} = \frac{L_c \times F}{W} \quad (8)$$

where L_c is the total length of chloroplast surface area facing the intercellular air space in the palisade tissue or spongy tissue sections.

The volume fraction of intercellular air space (f_{ias}) was determined as:

$$f_{ias} = 1 - \frac{\sum S_s}{t_{mes} \times W} \quad (9)$$

where t_{mes} is the mesophyll thickness between the two epidermal layers and ΣS_s is the sum of the cross-sectional areas of mesophyll cells.

The volume fraction of intercellular air space of palisade tissue and spongy tissue was determined respectively as:

$$f_{ias}(\text{palisade}) = 1 - \frac{\sum S_{pal}}{t_{pal} \times W} \quad (10)$$

$$f_{ias}(\text{spongy}) = 1 - \frac{\sum S_{spo}}{t_{spo} \times W} \quad (11)$$

Where ΣS_{pal} is the sum of the cross-sectional areas of palisade tissue cells, t_{pal} is the palisade tissue thickness, ΣS_{spo} is the sum of the cross-sectional areas of spongy tissue cells, t_{spo} is the spongy tissue thickness.

Chloroplast length (L_{chl}), chloroplast thickness (T_{chl}) and T_{cw} were obtained at different positions in each sample at ×30 000 magnifications. For a given section, all characteristics were determined in at least three different fields of view, and at least three different sections were analysed.

The cross-section of a chloroplast is assumed to be oval. Therefore, the cross-section area of chloroplast ($Area_{chl}$) was calculated in the palisade tissue or spongy tissue section as:

$$Area_{chl} = \pi \times L_{chl} \times T_{chl} \quad (12)$$

where π is the ratio of the circumference of a circle to its diameter.

g_m *modeled from anatomical characteristics*

According to the quantitative one-dimensional gas diffusion model of Niinemets and Reichstein (2003) further used by Tosens *et al.* (2016), mesophyll conductance of total leaf, palisade, spongy tissue and bract was estimated using the leaf anatomical characteristics (i.e. $g_{m(anatomy)}$). In the model, $g_{m(anatomy)}$ is separated into gas phase conductance and liquid phase conductance (Evans *et al.*, 1994):

$$g_{m(anatomy)} = \frac{1}{\frac{1}{g_{ias}} + \frac{R \times T_K}{H \times g_{liq}}} \quad (13)$$

where g_{ias} is conductance from substomatal cavities to outer surface of cell walls and g_{liq} is the conductance from outer surface of cell walls to chloroplasts; R is the gas constant (Pa m^3 K^{-1} mol^{-1}), H is the Henry's law constant (Pa m^3 mol^{-1}), and T_k is the absolute temperature (K). $H/(R \times T_k)$ is needed to convert g_{liq} to a gas phase equivalent conductance (Niinemets and Reichstein, 2003).

The gas phase conductance (g_{ias}) was calculated as described in Niinemets and Reichstein (2003):

$$g_{ias} = \frac{D_a \times f_{ias}}{\Delta L_{ias} \times \varsigma} \quad (14)$$

where ΔL_{ias} was taken as half the mesophyll thickness (Niinemets and Reichstein, 2003), D_a ($m^{-2}s^{-1}$) is the diffusion coefficient for CO_2 in the gas phase (1.51 × 10^{-5} m^{-2} s^{-1} at 25 °C), and ς is the diffusion path tortuosity (m m^{-1}) for which we used a default value of 1.57 m m^{-1} (Syvertsen *et al.*, 1995; Niinemets and Reichstein, 2003).

The total liquid phase conductance is provided by the sum of the inverse of serial conductances (Tosens *et al.*, 2016):

$$\frac{1}{g_{liq}} = \left(\frac{1}{g_{cw}} + \frac{1}{g_{pl}} + \frac{1}{g_{ct}} + \frac{1}{g_{en}} + \frac{1}{g_{st}}\right) \times \frac{S_c}{S} \quad (15)$$

where the partial conductances are those for cell wall (g_{cw}), plasmalemma (g_{pl}), cytosol (g_{ct}), chloroplast envelope (g_{en}), and chloroplast stroma (g_{st}). g_{cw}, g_{ct}, and g_{st} were calculated as described in Tomás *et al.* (2013). Cell wall porosity (p_{cw}) varied with T_{cw} according to Tosens *et al.* (2016) ($p_{cw} = -0.3733 \times T_{cw} + 0.3378$). We used an estimate of 0.0035 m s^{-1} for g_{pl} and g_{en} (Tosens *et al.*, 2012*b*). Conductance in units of m s^{-1} can be converted into molar units considering that:

$$g[\text{mol m}^{-2}\text{ s}^{-1}] = g[\text{m s}^{-1}] \times 44.6 \times \frac{273.15}{273.15 + T_L} \times \frac{P}{101.325}$$

where T_L is the leaf temperature (°C) and P (Pa) is the air pressure.

Quantitative analysis of partial limitation of g_m modeled

According to Tosens *et al.* (2016), the limitations derived from different components were calculated as:

$$L_{ias} = \frac{g_{m(anatomy)}}{g_{ias}} \quad (16)$$

$$L_i = \frac{g_{m(anatomy)}}{g_i \times \frac{S_c}{S}} \quad (17)$$

where $g_{m(anatomy)}$ is mesophyll conductance estimated from anatomical characteristics applying the model of Niinemets and Reichstein (2003) as modified by Tosens *et al.* (2016), L_{ias} is the limitation derived from the gas phase component, L_i is the component limitation in the cell wall, plasmalemma, cytoplasm, chloroplast envelope, and stroma, g_i refers to the component diffusion conductance of the corresponding diffusion pathways.

Relative limitation analyses on A_N

The relative limitation on A_N was analysed in cotton leaves and bracts. According to Grassi and Magnani (2005), relative stomatal limitation (l_s), mesophyll limitation (l_m), and biochemical limitation (l_b) were investigated in the cotton leaves and bracts. l_m was calculated using g_m calculated from gas-exchange plus fluorescence measurements following Harley *et al.* (1992*a*) ($g_{m(Harley)}$), from anatomical characteristics applying the model of Niinemets and Reichstein (2003) as modified by Tosens *et al.* (2016) ($g_{m(anatomy)}$) and from the average value between the anatomy and Harley methods. The relative changes in light-saturated assimilation can be expressed in terms of parallel relative changes in stomatal and mesophyll conductance and in biochemical capacity as follows:

$$\frac{dA_N}{A_N} = SL + MCL + BL = l_s \times \frac{dg_s}{g_s} + l_m \times \frac{dg_m}{g_m} + l_b \times \frac{dv_{cmax}}{v_{cmax}} \quad (18)$$

$$l_s = \frac{\frac{g_{tot}}{g_s} \times \frac{\partial A_N}{\partial C_c}}{g_{tot} + \frac{\partial A_N}{\partial C_c}} \quad (19)$$

$$l_m = \frac{\frac{g_{tot}}{g_m} \times \frac{\partial A_N}{\partial C_c}}{g_{tot} + \frac{\partial A_N}{\partial C_c}} \quad (20)$$

$$l_b = \frac{g_{tot}}{g_{tot} + \frac{\partial A_N}{\partial C_c}} \quad (21)$$

where g_{tot} is total conductance to CO_2 between the leaf surface and the sites of carboxylation ($1/g_{tot}=1/g_s+1/g_m$); l_s, l_m, and l_b are the corresponding relative limitation ($0<l_i<1$, i=s, m, b). Here, $\frac{\partial A_N}{\partial C_c}$ was calculated as the slope of A_N–C_c response curves over a C_c range of 50–100 μmol mol^{-1} (Tomás *et al.*, 2013)

Chlorophyll content, mass per area and nitrogen content

The chlorophyll content of leaves and bracts was determined in eight leaf discs (0.186 cm^2 each). Discs of the green organs were extracted in 80% (v/v) acetone for 24 h at room temperature in the dark. The absorbance of an extract was measured with a spectrophotometer, and the chlorophyll content was calculated according to Lichtenthaler (1987).

Leaf mass per unit area (LMA) is the ratio of dry weight and leaf area. Dry weight was determined from oven-dried certain area of leaf discs after 48 h at ca. 80 °C. Leaf density was defined as LMA divided by leaf thickness.

For the measurement of nitrogen content, leaves and bracts were harvested on the same day. Total nitrogen content of the dried tissues was determined according to the micro-Kjeldahl method (Schuman *et al.*, 1972).

Statistical analysis

Statistical analysis was performed with SPSS 17.0 for Windows (SPSS Inc., Chicago, IL, USA). All data were tested by analysis of variance (ANOVA). The significance of differences between treatment means was determined by the Student–Newman–Keuls (S-N-K) test at the 0.05 probability level. Data are presented as the means±standard error (SE) of three replicates.

Results

Difference in photosynthetic properties between cotton leaves and bracts

The net CO_2 assimilation rate (A_N), stomatal conductance (g_s), and mesophyll conductance (g_m) were significantly higher in leaves than in cotton bracts (Table 1). In cotton leaves the A_N response to increasing C_i initially increased, then peaked, and finally remained stable above 600 μmol mol^{-1} C_i. A_N as a function of C_i in cotton bracts was lower than that in leaves (Fig. 2A). Relative to leaves, A_N response to increasing PPFD in the bracts was minor and saturated at a lower irradiance (Fig. 2B). Both chlorophyll (a+b) content and the ratio between chlorophyll a and chlorophyll b (Chl$a$/b) of cotton bracts were much lower than those in the cotton leaves (Table 2). The nitrogen content of bracts was 21% lower than that of leaves (Table 2). Larger V_{cmax} and J_{max} derived from

Table 1. *Net assimilation rate (A_N), stomatal conductance (g_s), and mesophyll conductance (g_m) estimated by three independent methods: using gas-exchange plus fluorescence measurements following Harley et al. (1992a), the curve-fitting method of Sharkey (2016), and using g_m estimated from anatomical characteristics applying the model of Niinemets and Reichstein (2003) as modified by Tosens et al. (2016) in total leaves, palisade and spongy tissue of leaves, and bracts*

		A_N (μmol CO_2 m^{-2} s^{-1})	g_s (mol H_2O m^{-2} s^{-1})	$g_{m(Harley)}$ (mol CO_2 m^{-2} s^{-1})	$g_{m(Sharkey)}$ (mol CO_2 m^{-2} s^{-1})	$g_{m(anatomy)}$ (mol CO_2 m^{-2} s^{-1})
Leaf	Total	37.26 ± 1.93a	0.62 ± 0.07a	0.37 ± 0.01a	0.48 ± 0.10a	0.33 ± 0.03a
	Palisade tissue	–	–	–	–	0.25 ± 0.02b
	Spongy tissue	–	–	–	–	0.14 ± 0.02c
Bract	Total	3.58 ± 0.28b	0.06 ± 0.00b	0.03 ± 0.00b	0.05 ± 0.02b	0.11 ± 0.01c

Values are means±SE. Different letters indicate significant differences at the 0.05 probability level.

Table 2. *Chlorophyll* a+b *(chl(*a+b*)), the ratio between chlorophyll* a *and chlorophyll* b *(Chla/*b*), nitrogen (N) content (%), maximum carboxylation rate (V_{cmax}), and maximum electron transport rate (J_{max}) based on the chloroplastic CO_2 concentration (C_c) and electron transport rate from chlorophyll fluorescence (J_{flu}) calibrated by electron transport from gas exchange (J_A) under 2% O_2 conditions*

	Chl(*a+b*) (mg dm^{-2})	**Chla/*b* (%)**	**N content (%)**	**$V_{cmax\text{-}Cc}$ (μmol m^{-2} s^{-1})**	**$J_{max\text{-}Cc}$ (μmol m^{-2} s^{-1})**	**J_{flu} (μmol m^{-2} s^{-1})**
Leaf	5.73 ± 0.25a	3.14 ± 0.21a	3.62 ± 0.44a	526.7 ± 65.0a	456.0 ± 68.0a	345.4 ± 24.3a
Bract	2.15 ± 0.17b	2.51 ± 0.08b	2.86 ± 0.07b	39.3 ± 9.0b	52.0 ± 7.9b	55.0 ± 0.5b

Values are means±SE. Different letters indicate significant differences at the 0.05 probability level.

A_N–C_c curves were observed in the leaf than in the bract. The electron transport rate from chlorophyll fluorescence (J_{flu}) calibrated by electron transport from gas exchange (J_A) under 2% O_2 conditions was close to J_{max} based on the C_c. There was a difference in A_N, $A_{N\text{-}chl}$, and $A_{N\text{-}N}$ as a function of C_c between leaves and bracts (Fig. 3A–C).

At the low values found in bracts, the accuracy of the estimates of g_m is low and the photosynthesis limitation analysis is very sensitive to small variation in any of its input parameters. Consequently, the results of the limitation analysis were completely different depending on which estimate we used (Fig. 4; Supplementary Fig. S2). Still, the Harley and the anatomy methods rely on completely independent assumptions (they have no single assumption in common), and yet both indicated low g_m in bracts (see the anatomy method results in the next section). Because of the aforementioned accuracy problems, the absolute values, however, have to be taken with caution. The 'real' values would very likely be somewhere in between the two extremes represented by the Harley method on the one hand and the anatomy-based estimates on the other. For this reason we used the average of both methods to run the photosynthesis limitation analysis (Fig. 4). There was no significant difference between l_m based on the average g_m between the anatomy and Harley methods and l_s in bracts (Fig. 4). However, l_b was higher than l_s and l_m in bracts (Fig. 4). Leaves had the same level of l_s, l_m, and l_b (Fig. 4).

Anatomical measurements of cotton leaves and bracts

In the C_3 cotton leaves, two types of chlorenchyma are found, palisade tissue and spongy tissue. In order to compare the structural differences between leaf and bract, palisade and spongy tissue of leaf and bract were quantified separately. In leaves, mesophyll tissue is differentiated into palisade and spongy mesophyll, the palisade tissue being more compact with a lower porosity (f_{ias}; see Supplementary Fig. S3A, B). However, in the cotton bract, only one type of tissue was found, which was similar to the leaf spongy mesophyll (Fig. S3A, B). Although the LMA, leaf thickness (T) and density (D) in the cotton leaf were significantly higher than those in the bract (Table 3), we observed that there were no differences in the S_m/S, S_c/S, chloroplast thickness (T_{chl}) and $Area_{chl}$ between spongy tissue of leaves and bracts (Table 3). Bracts had higher f_{ias} and cell wall thickness (T_{cw}) than spongy tissue of leaves (Table 3). The spongy tissue of leaves and bracts also showed similar anatomical structure (Fig. S3). Quantitative limitations of g_m modeled by anatomy were estimated according to the component diffusion conductance of the corresponding diffusion pathways

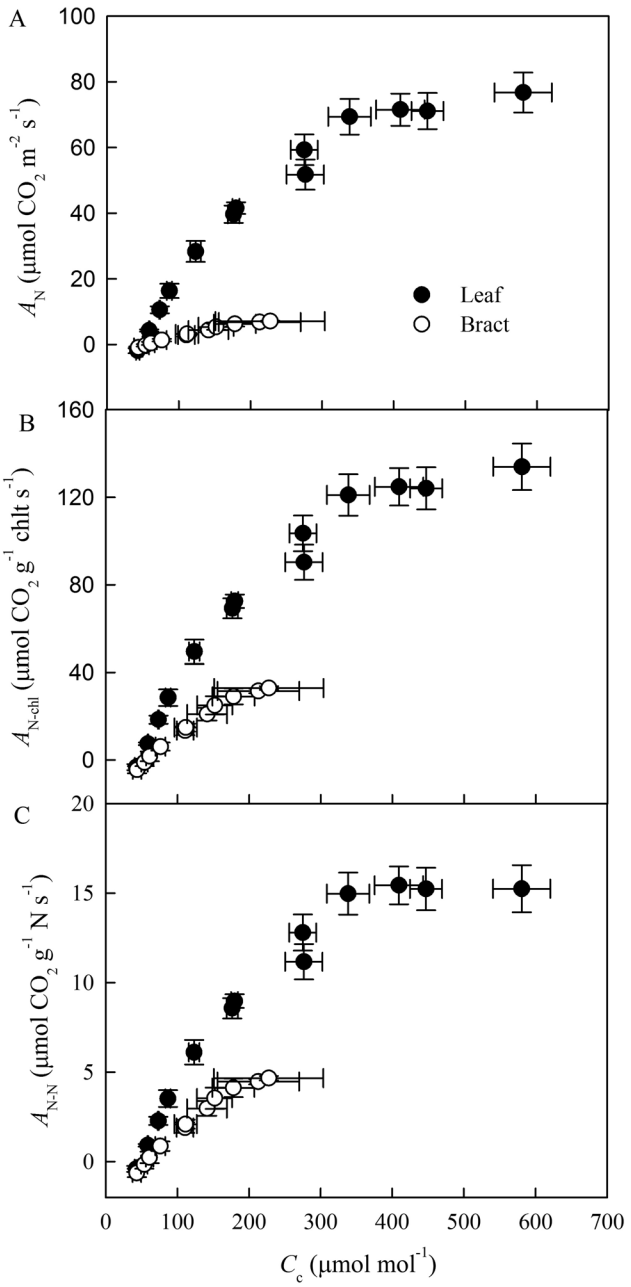

Fig. 3. Net CO_2 assimilation rate expressed on the basis of area (A_N) (A), chlorophyll ($a+b$) ($A_{N\text{-}chl}$) (B), and nitrogen content ($A_{N\text{-}N}$) (C) as a function of chloroplastic CO_2 concentration (C_c) in cotton leaves and bracts. Values are means±SE.

(Fig. 5). The limitation derived from the gas phase components (L_{ias}) (5–34%) was lower than the total limitation from liquid phase components. In the liquid phase, the palisade and

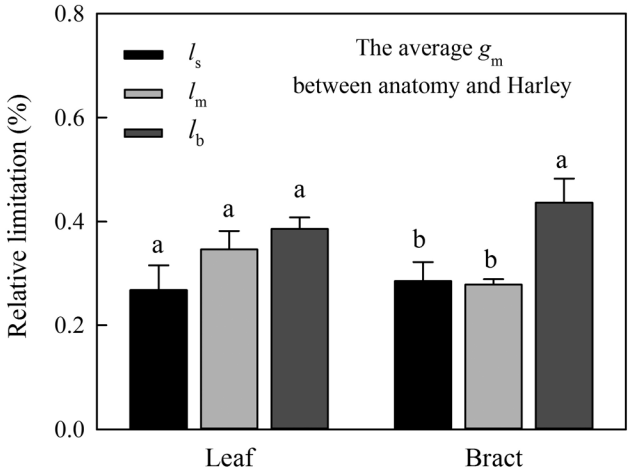

Fig. 4. Relative limitation analysis of photosynthesis in the leaves and bracts of cotton under normal ambient conditions. The total relative photosynthetic limitation was composed of stomatal (l_s), mesophyll conductance (l_m), and biochemical limitation (l_b). l_m was calculated using the average g_m between the anatomy and Harley methods. Values are means±SE. Different letters indicate significant differences between l_s, l_m, and l_b at the 0.05 probability level.

spongy tissue of leaves revealed the highest limitation by the stroma (L_s) of around 50%. There was no significant difference in the L_s between palisade and spongy tissue of leaves and bracts. In bracts, cell walls accounted for up to 50% of the limitations, compared with only 11% and 16% in palisade tissue and spongy tissue, respectively. The limitations derived from plasmalemma (L_p) and chloroplast envelop (L_e) in bracts were lower than those in spongy tissues, but were similar to those of palisade tissues of leaves.

Discussion

Lower A_N in bracts than in leaves is due to co-limiting CO_2 diffusion and biochemistry

It is well known that leaves are the main photosynthetic organs in plant species, but numerous researchers have shown that non-leaf green organs are also an important source of assimilated carbon (Tambussi *et al.*, 2007; Redondo-Gómez *et al.*, 2010; Pengelly *et al.*, 2011; Hu *et al.*, 2013; Jia *et al.*, 2015; Zhang *et al.*, 2015) and make a considerable contribution to terrestrial carbon exchange. In the case of cotton, bracts also have a photosynthetic function and contribute to carbon gain (Zhang *et al.*, 2010; Hu *et al.*, 2012, 2013). Moreover, it has been shown that some non-leaf green organs also have a strong stress tolerance, such as salt tolerance of rosette bracts (Redondo-Gómez *et al.*, 2010) and drought tolerance of cotton bracts (Zhang *et al.*, 2015) and wheat ears (Jia *et al.*, 2015). Hence, it is possible that, under abiotic stress conditions, non-leaf green organs make a considerable contribution to the carbon cycle.

Despite their importance, no previous study has focused on photosynthetic limitations and their anatomical basis in cotton bracts. In our study, A_N expressed on an area basis in bracts saturated at low irradiance (Fig. 2B; 3.58 μmol CO_2 m^{-2} s^{-1}), suggesting that light intensity was not the most important limiting

Table 3 *Leaf mass per unit area (LMA), leaf thickness (T), density (D), mesophyll thickness (T_{mes}), the surface of mesophyll cells and chloroplasts exposed to leaf intercellular air spaces (S_m/S and S_c/S; μm^2 μm^{-2}), the chloroplast thickness, the thickness of the cytoplasm between the cell membrane and the chloroplast (T_{cyt}), the cross-section area of chloroplast ($Area_{chl}$), the volume fraction of intercellular air space (f_{ias}) and cell wall thickness (T_{cw}) in the cotton leaves and bracts*

		LMA (g m^{-2})	T (μm)	D (g cm^{-3})	T_{mes} (μm)	S_m/S	S_c/S	T_{chl} (μm)	T_{cyt} (μm)	$Area_{chl}$ (μm^2)	f_{ias} (%)	T_{cw} (μm)
Leaf	Total	128.2 ± 0.5a	411 ± 10.2a	0.32 ± 0.00a	375 ± 6.6a	39.96 ± 2.3a	29.66 ± 2.5a	1.79 ± 0.28a	0.24 ± 0.07a	26.45 ± 4.1b	0.47 ± 0.02c	0.18 ± 0.01b
	Palisade tissue	–	–	–	195 ± 2.5c	28.9 ± 0.3b	22.6 ± 0.9b	2.22 ± 0.47a	0.34 ± 0.11a	37.81 ± 3.4a	0.33 ± 0.03d	0.20 ± 0.01b
	Spongy tissue	–	–	–	173 ± 4.2c	11.1 ± 2.1c	7.1 ± 0.9c	1.35 ± 0.15a	0.14 ± 0.09a	18.51 ± 2.1c	0.60 ± 0.01b	0.17 ± 0.01b
Bract	Total	53.1 ± 2.4b	350 ± 18.8b	0.15 ± 0.01b	300 ± 18.0b	14.6 ± 0.3c	7.4 ± 0.6c	1.12 ± 0.12a	0.13 ± 0.02a	15.65 ± 1.3c	0.75 ± 0.02a	0.45 ± 0.02a

Values were means±SE. Different letters indicate significant differences at the 0.05 probability level.

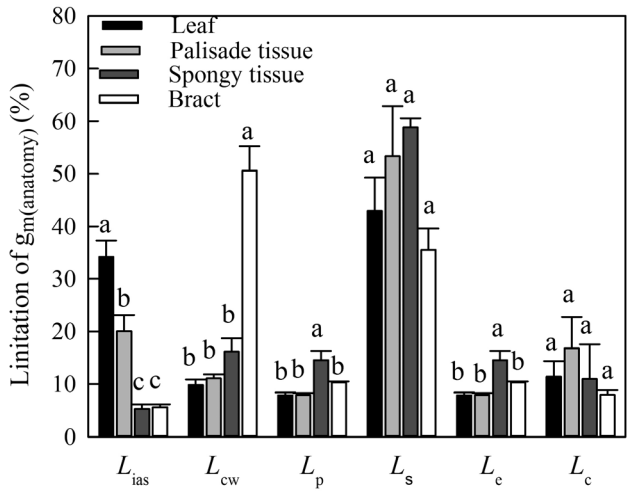

Fig. 5. Quantitative analysis of partial limitation of mesophyll conductance modeled ($g_{m(anatomy)}$) in the palisade and spongy tissue of leaves and the bracts. L_{ias}, the limitation derived from the gas phase components; L_{cw}, the limitation derived from the cell wall; L_p, the limitation derived from the plasmalemma; L_s, the limitation derived from the stroma; L_e, the limitation derived from the chloroplast envelope; L_c, the limitation derived from the cytoplast. Different letters indicate significant differences between palisade, spongy and bracts at the 0.05 probability level.

factor for bract photosynthesis. It is likely that bracts can tolerate and thrive in low light intensity due to their growth in a shaded position over an evolutionary time of at least 1.1 million years since the appearance of tetraploid cotton (Hu *et al.*, 2013). A lower Chl*a*/*b* (Table 1) in the bract may be also a long-term adaption to capture more light. Björkman (1981) also suggested controlling the Chl*a*/*b* is one way to adapt the photosynthetic function to light.

The high values of photosynthesis observed in cotton leaves in this study (Table 1) were similar to those already reported for this species (Ephrath *et al.*, 1990; Faver and Gerik, 1996). Consequently, net CO_2 assimilation rate (A_N) values in cotton bracts were 90% lower than those obtained for leaves (Table 1; Fig. 2), which is accompanied by lower values of all the parameters related to photosynthesis. g_s in bracts was only about 10% that of leaves, g_m 8–36% (depending on which g_m estimate was used), V_{cmax} 7.5% and J 11–16% (depending on whether considering J_{max} or J_{flu}). In this study, g_m was estimated by three independent methods that gave similar results for leaves, but this similarity was not found in bracts, with a significantly higher $g_{m(anatomy)}$ than $g_{m(Harley)}$ (Table 1). This may be partly due to the estimation biases of the currently available techniques. For instance, the variable J method was influenced by accuracy of C_i estimation (Gu and Sun, 2014) and (photo) respiratory CO_2 recycling (Tholen *et al.*, 2012). We did our best to ensure the accuracy of C_i through calibration. Although the variable J method cannot rule out the effect of (photo) respiratory CO_2 recycling, it is unlikely that this alone causes such a big difference in $g_{m(Harley)}$ between leaf and bract and between $g_{m(anatomy)}$ and $g_{m(Harley)}$. In addition, the estimation of $g_{m(anatomy)}$ is also subject to uncertainties. For instance, variable cell wall porosity was considered as a function of cell wall thickness (see 'Materials and methods' and Tosens *et al.*, 2016). But there was still a highly apparent discrepancy or inconsistency between $g_{m(anatomy)}$ and $g_{m(Harley)}$, and the difference in $g_{m(anatomy)}$ between leaf and bract could not account for the observed difference in photosynthesis (Table 1). The overestimation of $g_{m(anatomy)}$ in the bract could be because the anatomical model does not account for variations in some biochemical properties (e.g. the expression of aquaporins and carbonic anhydrase) that might be involved in the CO_2 diffusion. In our experiment, a conservative constant value (0.0035 m s^{-1}) was used to estimate the g_{pl} and g_{en} as suggested in Evans *et al.* (1994) and Tosens *et al.* (2012*a*), but membrane permeability is affected by the expression of aquaporins and varies among different organs, species, and environments. In order to test the role of membrane permeability, we tried different values that have been reported in the literature (see Table 1 in Evans *et al.*, 2009). When g_{pl} and g_{en} in the bract were replaced by 0.0008 m s^{-1} (which is the permeability reported for yeast cells), $g_{m(anatomy)}$ was 0.069 mol CO_2 m^{-2} s^{-1}, i.e. much closer to $g_{m(Harley)}$. Therefore, membrane permeability can be another potential cause of (i) the huge difference in photosynthesis between leaf and bract, and (ii) the discrepancy between $g_{m(anatomy)}$ and $g_{m(Harley)}$. This is why, considering that the actual value may be somewhere in between the extremes of the estimations, we have used the average g_m between anatomy and Harley values for the limitation analyses on photosynthesis. Both the similarity in the reductions of all the parameters related to photosynthesis (Table 1) and the relative limitation analysis (Fig. 4) confirmed that CO_2 diffusion and biochemistry co-limit bract photosynthesis in a similar way. High biochemical limitation in bracts could be caused by a low Rubisco activity, as Bota *et al.* (2004) proved its good agreement with V_{cmax} derived from A_N–C_c curves. Bracts had very low g_s, and high stomatal limitation would be likely due to the limited hydraulic capacity caused by the low main vein density.

Subcellular anatomical traits play important roles in setting g_m of bracts

Leaf mass per unit area (LMA) is an integrative trait of leaf structural characteristics affecting g_m. It is mainly dependent on leaf thickness and density (Niinemets, 2015). John *et al.* (2017) reported that the number of cell layers and cell volume that is associated with leaf thickness and density are among the most important intrinsic drivers of LMA. Because leaf thickness and density are closely related to the S_c/S and T_{cw}, theoretically LMA has an important role in setting g_m. Leaf thickness was 1.25 times larger than bract thickness and leaf density was 1.89 times larger than bract density (Table 3). These results suggest that higher density in the leaf mainly contributed to larger LMA. A lower proportion of mesophyll and a higher f_{ias} due to random cell arrangement and lower cell numbers led to lower density in bracts (Table 3; Supplementary Fig. S3). While early studies have shown that there is a negative relationship between LMA and g_m across broad functional groups and within species (Flexas *et al.*, 2008; Niinemets *et al.*, 2009; Galmés *et al.*, 2011; Tosens *et al.*, 2016), this is not consistent with our results, which show that bracts have lower LMA than leaves despite having a higher T_{cw} (Table 3). Recently, Onoda *et al.* (2017) highlighted that subcellular anatomical traits such as T_{cw}, S_m/S,

and S_c/S are much more important than LMA in setting g_m. Similarly, Peguero-Pina *et al.* (2017) showed that these parameters as well as f_{ias} can mask the effects of LMA on g_m.

CO_2 diffuses from the intercellular air spaces to the sites of carboxylation within chloroplasts in gas phases largely affected by leaf porosity, reflected by f_{ias} (Hanba *et al.*, 1999), and liquid phases largely affected by T_{cw}, S_m/S, and S_c/S (Evans *et al.*, 1994; Hanba *et al.*, 2004; Terashima *et al.*, 2011; Tomás *et al.*, 2013; Peguero-Pina *et al.*, 2016). Evans *et al.* (1994) concluded that g_{ias} is so large that it is not a major determinant of g_m in leaves. Instead, T_{cw}, S_m/S, and S_c/S, which affect g_{liq}, are considered the main determinants of differences in g_m among species (Terashima *et al.*, 2011; Tomás *et al.*, 2013; Peguero-Pina *et al.*, 2016, 2017). Bracts with thin mesophyll thickness had smaller S_m/S and S_c/S than leaves (Table 2). Several studies have indicated larger S_m/S and S_c/S in thicker leaves (Hanba *et al.*, 1999; Terashima *et al.*, 2006; Peguero-Pina *et al.*, 2016), likely reflecting the more developed palisade tissues in the thicker leaves. The smaller S_m/S and S_c/S were also likely due to higher f_{ias} that was caused by the fewer and smaller cells in bracts. Based on this, we quantified separately the anatomical structure of palisade and spongy tissues in leaves (Table 3). The quantitative results indicated that S_m/S and S_c/S of bracts were similar to the spongy tissue of leaves, which contributed to lower g_m in bracts and the spongy tissue of the leaves. In addition, chloroplast size and thickness are also an important factor limiting CO_2 diffusion to Rubisco (Tomás *et al.*, 2013; Tosens *et al.*, 2016; Veromann-Jürgenson *et al.*, 2017), and thus smaller $Area_{chl}$ in bracts and the spongy tissue of the leaves was also a cause of lower g_m. Although numerous studies reported that T_{cw} is generally higher in woody species with thick leaves (Evans *et al.*, 2009; Terashima *et al.*, 2011; Tosens *et al.*, 2012*b*; Veromann-Jürgenson *et al.*, 2017), higher T_{cw} was observed in bracts than in either the palisade or spongy tissues of leaves. This is possibly due to a larger nitrogen investment in structural construction (i.e. the cell wall construction) in bracts than in leaves, which is supported by lower $A_{N\text{-}N}$ expressed on the basis of nitrogen content in bracts (Fig. 3C). In this sense, relative to leaves, a larger nitrogen investment in cell wall construction led to lower g_m in bracts. Instead, mesophyll conductance of bracts was similar to that of spongy tissues, the highest values being those of palisade tissue. The further anatomical limitation analysis (Fig. 5) showed that the limitation derived from the cell wall (L_{cw}) is higher in bracts than in spongy tissue, but the cumulative effects of subtle differences in each subcellular structure, especially the chloroplast traits, compensate L_{cw} to yield similar g_m in bracts and spongy tissue. However, there was smaller g_m in bracts than in palisade tissue because of the larger T_{cw}, greater f_{ias}, smaller chloroplasts, and lower S_m/S and S_c/S.

Conclusion

In summary, net CO_2 assimilation rate (A_N) was lower in cotton bracts than in leaves, and this was due to concomitant and similar limitations by biochemistry, stomatal conductance (g_s), and mesophyll diffusion conductance (g_m). Concerning g_m, we provide the first report showing that anatomical traits setting the limits for g_m in leaves also operate in non-leaf photosynthetic tissues like bracts. Specifically, larger T_{cw} and f_{ias}, smaller and fewer chloroplasts, lower S_m/S and S_c/S, and, perhaps, smaller membrane permeability in bracts than in leaves led to lower g_m. It has been shown that in leaves of angiosperm species (Flexas, 2016), but especially in crops (Nadal and Flexas, submitted), stomatal, mesophyll conductance and biochemical limitations to photosynthesis are of similar magnitude, for which significantly improving leaf photosynthetic capacity in crops cannot be achieved unless all three factors are improved (Flexas, 2016). Here we show that this might be similar in bracts. Since bracts contribute significantly to the photosynthetic carbon gain of plants (Zhang *et al.*, 2010, Hu *et al.*, 2012, 2013), the present results should be considered in future attempts to improve crop productivity by means of manipulating photosynthesis.

Supplementary data

Supplementary data are available at *JXB* online.

Fig. S1. Daily maximum and minimum air temperature and precipitation during the growing season at the experimental field.

Fig. S2. Relative limitation analysis of photosynthesis for leaves and bracts of cotton under ambient conditions.

Fig. S3. Light and electron microscopy images of cotton leaves and bracts.

Acknowledgements

This work was supported by the National Natural Science Foundation of China (Grant No. U1303183), Program for the Excellent Youth Scholar of Higher Education of XPCC (CZ027201) and Plan for Training Youth Innovative Talent in Shihezi University (CXRC201701). The authors also thank the China Scholarship Council (CSC) for the funding of joint training PhD.

References

Bernacchi CJ, Portis AR, Nakano H, von Caemmerer S, Long SP. 2002. Temperature response of mesophyll conductance. Implications for the determination of Rubisco enzyme kinetics and for limitations to photosynthesis in vivo. Plant Physiology **130,** 1992–1998.

Björkman O. 1981. Responses to different quantum flux densities. In: Lange OL, Nobel PS, Osmond CB, Ziegler H, eds. Physiological Plant Ecology I. Encyclopedia of Plant Physiology (New Series). Berlin, Heidelberg: Springer.

Bota J, Medrano H, Flexas J. 2004. Is photosynthesis limited by decreased Rubisco activity and RuBP content under progressive water stress? New Phytologist **162,** 671–681.

Ephrath J, Marani A, Bravdo BA. 1990. Effect of moisture stress on stomatal resistance and photosynthetic rate in cotton (*Gossypium hirsutum* L.): controlled level of stress. Field Crops Research **23,** 117–131.

Ethier GJ, Livingston NJ. 2004. On the need to incorporate sensitivity to CO_2 transfer conductance into the Farquhar–von Caemmerer–Berry leaf photosynthesis model. Plant, Cell & Environment **27,** 137–153.

Evans JR, Kaldenhoff R, Genty B, Terashima I. 2009. Resistances along the CO_2 diffusion pathway inside leaves. Journal of Experimental Botany **60,** 2235–2248.

Evans JR, Von Caemmerer S, Setchell BA, Hudson GS. 1994. The relationship between CO_2 transfer conductance. Australian Journal of Plant Physiology **21,** 475–495.

Farquhar GD, von Caemmerer S, Berry JA. 1980. A biochemical model of photosynthetic CO_2 assimilation in leaves of C_3 species. Planta **149,** 78–90.

Faver KL, Gerik TJ. 1996. Foliar-applied methanol effects on cotton (*Gossypium hirsutum* L.) gas exchange and growth. Field Crops Research **47,** 227–234.

Flexas J, Barbour MM, Brendel O, *et al*. 2012. Mesophyll diffusion conductance to CO2: An unappreciated central player in photosynthesis. Plant Science **193–194,** 70–84.

Flexas J. 2016. Genetic improvement of leaf photosynthesis and intrinsic water use efficiency in C_3 plants: Why so much little success? Plant Science **251,** 155–161.

Flexas J, Diaz-Espejo A, Galmés J, Kaldenhoff R, Medrano H, Ribas-Carbo M. 2007. Rapid variations of mesophyll conductance in response to changes in CO_2 concentration around leaves. Plant, Cell & Environment **30,** 1284–1298.

Flexas J, Ribas-Carbó M, Diaz-Espejo A, Galmés J, Medrano H. 2008. Mesophyll conductance to CO_2: current knowledge and future prospects. Plant, Cell & Environment **31,** 602–621.

Galmés J, Andralojc PJ, Kapralov MV, Flexas J, Keys AJ, Molins A, Parry MA, Conesa MÀ. 2014. Environmentally driven evolution of Rubisco and improved photosynthesis and growth within the C_3 genus *Limonium* (Plumbaginaceae). New Phytologist **203,** 989–999.

Galmés J, Conesa MÀ, Ochogavía JM, Perdomo JA, Francis DM, Ribas-Carbó M, Savé R, Flexas J, Medrano H, Cifre J. 2011. Physiological and morphological adaptations in relation to water use efficiency in Mediterranean accessions of *Solanum lycopersicum*. Plant, Cell & Environment **34,** 245–260.

Grassi G, Magnani F. 2005. Stomatal, mesophyll conductance and biochemical limitations to photosynthesis as affected by drought and leaf ontogeny in ash and oak trees. Plant, Cell & Environment **28,** 834–849.

Gu L, Pallardy SG, Tu K, Law BE, Wullschleger SD. 2010. Reliable estimation of biochemical parameters from C_3 leaf photosynthesis–intercellular carbon dioxide response curves. Plant, Cell & Environment **33,** 1852–1874.

Gu L, Sun Y. 2014. Artefactual responses of mesophyll conductance to CO_2 and irradiance estimated with the variable *J* and online isotope discrimination methods. Plant, Cell & Environment **37,** 1231–1249.

Hanba YT, Shibasaka M, Hayashi Y, Hayakawa T, Kasamo K, Terashima I, Katsuhara M. 2004. Overexpression of the barley aquaporin HvPIP2;1 increases internal CO_2 conductance and CO_2 assimilation in the leaves of transgenic rice plants. Plant & Cell Physiology **45,** 521–529.

Hanba YT, Miyazawa SI, Terashima I. 1999. The influence of leaf thickness on the CO_2 transfer. Functional Ecology **13,** 632–639.

Harley PC, Loreto F, Di Marco G, Sharkey TD. 1992*a*. Theoretical considerations when estimating the mesophyll conductance to CO_2 flux by analysis of the response of photosynthesis to CO_2. Plant Physiology **98,** 1429–1436.

Harley PC, Thomas RB, Reynolds JF, Strain BR. 1992*b*. Modelling photosynthesis of cotton grown in elevated CO_2. Plant, Cell & Environment **15,** 271–282.

Hu YY, Oguchi R, Yamori W, von Caemmerer S, Chow WS, Zhang WF. 2013. Cotton bracts are adapted to a microenvironment of concentrated CO_2 produced by rapid fruit respiration. Annals of Botany **112,** 31–40.

Hu YY, Zhang YL, Luo HH, Li W, Oguchi R, Fan DY, Chow WS, Zhang WF. 2012. Important photosynthetic contribution from the non-foliar green organs in cotton at the late growth stage. Planta **235,** 325–336.

Jia S, Jiang S, Liang T, Liu C, Jing Z. 2015. Response of wheat ear photosynthesis and photosynthate carbon distribution to water deficit. Photosynthetica **53,** 95–109.

John GP, Scoffoni C, Buckley TN, Villar R, Poorter H, Sack L. 2017. The anatomical and compositional basis of leaf mass per area. Ecology Letters **20,** 412–425.

Lichtenthaler HK. 1987. Chlorophylls and carotenoids: pigments of photosynthetic biomembranes. Methods in Enzymology **148,** 350–382.

Miao Z, Xu M, Lathrop RG Jr, Wang Y. 2009. Comparison of the A–C_c curve fitting methods in determining maximum ribulose 1.5-bisphosphate carboxylase/oxygenase carboxylation rate, potential light saturated electron transport rate and leaf dark respiration. Plant, Cell & Environment **32,** 109–122.

Niinemets Ü. 2007. Photosynthesis and resource distribution through plant canopies. Plant, Cell & Environment **30,** 1052–1071.

Niinemets Ü. 2015. Is there a species spectrum within the world-wide leaf economics spectrum? Major variations in leaf functional traits in the Mediterranean sclerophyll *Quercus ilex*. New Phytologist **205,** 79–96.

Niinemets Ü, Cescatti A, Rodeghiero M, Tosens T. 2005. Leaf internal diffusion conductance limits photosynthesis more strongly in older leaves of Mediterranean evergreen broad-leaved species. Plant, Cell & Environment **28,** 1552–1566.

Niinemets U, Díaz-Espejo A, Flexas J, Galmés J, Warren CR. 2009. Importance of mesophyll diffusion conductance in estimation of plant photosynthesis in the field. Journal of Experimental Botany **60,** 2271–2282.

Niinemets Ü, Reichstein M. 2003. Controls on the emission of plant volatiles through stomata: A sensitivity analysis. Journal of Geophysical Research **108,** D7.

Onoda Y, Wright IJ, Evans JR, Hikosaka K, Kitajima K, Niinemets Ü, Poorter H, Tosens T, Westoby M. 2017. Physiological and structural tradeoffs underlying the leaf economics spectrum. New Phytologist **214,** 1447–1463.

Peguero-Pina JJ, Sisó S, Flexas J, Galmés J, García-Nogales A, Niinemets Ü, Sancho-Knapik D, Saz MÁ, Gil-Pelegrín E. 2017. Cell-level anatomical characteristics explain high mesophyll conductance and photosynthetic capacity in sclerophyllous Mediterranean oaks. New Phytologist **214,** 585–596.

Peguero-Pina JJ, Sisó S, Sancho-Knapik D, Díaz-Espejo A, Flexas J, Galmés J, Gil-Pelegrín E. 2016. Leaf morphological and physiological adaptations of a deciduous oak (*Quercus faginea* Lam.) to the Mediterranean climate: a comparison with a closely related temperate species (*Quercus robur* L.). Tree Physiology **36,** 287–299.

Pengelly JJ, Kwasny S, Bala S, Evans JR, Voznesenskaya EV, Koteyeva NK, Edwards GE, Furbank RT, von Caemmerer S. 2011. Functional analysis of corn husk photosynthesis. Plant Physiology **156,** 503–513.

Pons TL, Flexas J, von Caemmerer S, Evans JR, Genty B, Ribas-Carbo M, Brugnoli E. 2009. Estimating mesophyll conductance to CO_2: methodology, potential errors, and recommendations. Journal of Experimental Botany **60,** 2217–2234.

Redondo-Gómez S, Mateos-Naranjo E, Moreno FJ. 2010. Physiological characterization of photosynthesis, chloroplast ultrastructure, and nutrient content in bracts and rosette leaves from *Glaucium flavum*. Photosynthetica **48,** 488–493.

Schuman GE, Stanley MA, Knudsen D. 1972. Automated total nitrogen analysis of soil and plant samples. Soil Science Society of America **37,** 480–481.

Sharkey TD. 2016. What gas exchange data can tell us about photosynthesis. Plant, Cell & Environment **39,** 1161–1163.

Sharkey TD, Bernacchi CJ, Farquhar GD, Singsaas EL. 2007. Fitting photosynthetic carbon dioxide response curves for C_3 leaves. Plant, Cell & Environment **30,** 1035–1040.

Sun Y, Gu LH, Dickinson RE, Norby RJ, Pallardy SG, Hoffman FM. 2014. Impact of mesophyll diffusion on estimated global land CO_2 fertilization. Proceedings of the National Academy of Sciences, USA **111,** 15774–15779.

Syvertsen JP, Lloyd J, McConchie C, Kriedemann PE, Farquhar GD. 1995. On the relationship between leaf anatomy and CO_2 diffusion through the mesophyll of hypostomatous leaves. Plant, Cell & Environment **18,** 149–157.

Tambussi EA, Bort J, Guiamet JJ, Nogues S, Araus JL. 2007. The photosynthetic role of ears in C3 cereals: metabolism, water use efficiency and contribution too grain yield. Critical Reviews in Plant Sciences **26,** 1–16.

Terashima I, Hanba YT, Tazoe Y, Vyas P, Yano S. 2006. Irradiance and phenotype: comparative eco-development of sun and shade leaves in relation to photosynthetic CO_2 diffusion. Journal of Experimental Botany **57,** 343–354.

Terashima I, Hanba YT, Tholen D, Niinemets Ü. 2011. Leaf functional anatomy in relation to photosynthesis. Plant Physiology **155,** 108–116.

Terashima I, Ishibashi M, Ono K, Hikosaka K. 1995. Three resistances to CO_2 diffusion: Leaf-surface water, intercellular spaces and mesophyll cells. In Mathis P, ed. Photosynthesis: From light to biosphere, vol. V. Norwell, MA, USA: Kluwer Academic, 537–542.

Thain JF. 1983. Curvature correction factors in the measurement of cell surface areas in plant tissues. Journal of Experimental Botany **34,** 87–94.

Tholen D, Ethier G, Genty B, Pepin S, Zhu XG. 2012. Variable mesophyll conductance revisited: theoretical background and experimental implications. Plant, Cell & Environment **35,** 2087–2103.

Tomás M, Flexas J, Copolovici L, Galmés J, Hallik L, Medrano H, Ribas-Carbó M, Tosens T, Vislap V, Niinemets Ü. 2013. Importance of leaf anatomy in determining mesophyll diffusion conductance to CO_2 across species: quantitative limitations and scaling up by models. Journal of Experimental Botany **64,** 2269–2281.

Tosens T, Niinemets U, Vislap V, Eichelmann H, Castro Díez P. 2012*a*. Developmental changes in mesophyll diffusion conductance and photosynthetic capacity under different light and water availabilities in *Populus tremula*: how structure constrains function. Plant, Cell & Environment **35,** 839–856.

Tosens T, Niinemets Ü, Westoby M, Wright IJ. 2012*b*. Anatomical basis of variation in mesophyll resistance in eastern Australian sclerophylls: news of a long and winding path. Journal of Experimental Botany **63,** 5105–5119.

Tosens T, Nishida K, Gago J, Coopman RE, Cabrera HM, Carriqui M, Laanisto L, Morales L, Nadal M, Rojas R. 2016. The photosynthetic capacity in 35 ferns and fern allies: mesophyll CO_2 diffusion as a key trait. New Phytologist **209,** 1576–1590.

Veromann-Jürgenson LL, Tosens T, Laanisto L, Niinemets Ü. 2017. Extremely thick cell walls and low mesophyll conductance: welcome to the world of ancient living! Journal of Experimental Botany **68,** 1639–1653.

Villar R, Held AA, Merino J. 1995. Dark leaf respiration in light and darkness of an evergreen and a deciduous plant species. Plant Physiology **107,** 421–427.

Zhang C, Zhan DX, Luo HH, Zhang YL, Zhang WF. 2015. Photorespiration and photoinhibition in the bracts of cotton under water stress. Photosynthetica **54,** 12–18.

Zhang YL, Feng GY, Hu YY, Yao YD, Zhang WF. 2010. Photosynthetic activity and its correlation with matter production in non-foliar green organs of cotton. Acta Agronomica Sinica **36,** 701–708. [Chinese with English abstract.]